

G
70.215
.02
D3
1981-6
ong6e

DAD Technical Note 1981-06

Noise Considerations for the
ESA-ERS-1 Doppler Scatterometer



L. Gray
Data Acquisition Division
Canada Centre for Remote Sensing
Ottawa, Ontario, Canada

July 1981

This document was produced
by scanning the original publication.
Ce document est le produit d'une
numérisation par balayage
de la publication originale.

Noise Considerations for the ESA ERS-1 Doppler Scatterometer

L. Gray

Abstract

Trade-offs between power, thermal noise, measurement accuracy, incoherent averaging, resolution, antenna beamwidths, etc. are required for optimization studies of the ESA ERS-1 Doppler Scatterometer. These notes and graphs present some of that information and make some observations and recommendations for follow-on work to the Dornier phase A scatterometer study*.

Contents

1. Standard Deviation in backscatter coefficient σ^0 measurement.
2. Doppler Bandwidth as a function of earth incidence angle (θ_i).
3. Number of independent samples as a function of θ_i .
4. K_p as a function of signal-to-noise ratio (SNR).
5. K_p for V and H Pol. ($\theta_i = 55^\circ$), comparison with SEASAT.
6. SNR as a function of θ (wind speed $u^* = 4, 8, 16 \text{ m sec}^{-1}$).
7. K_p as a function of θ .
8. Standard deviation in u^* as a function of θ and u^* .
9. Conclusions and Comments.

¹ "Satellite Scatterometer Feasibility Study",
Midterm Presentation, November 1980
Final Presentation, January 1981.

1) The Standard Deviation in Backscatter Coefficient (σ^0) Measurement

This is given by^{2, 3};

$$K_p = (\text{standard deviation in } \sigma^0 \text{ measurement}) / \sigma^0$$

$$K_p = \left\{ \frac{1}{(B_c \tau_{sn})} \left[1 + \frac{2}{SNR} + \frac{1}{(SNR)^2} \right] + \frac{1}{(B_c \tau_n)} \cdot \frac{1}{(SNR)^2} \right\}^{\frac{1}{2}}$$

when τ_n (total noise measurement period) = $(2 \tau_{sn})$, where τ_{sn} is the total signal plus noise measurement period

then

$$K_p = \frac{1}{\sqrt{B_c \tau_{sn}}} \left\{ 1 + \frac{2}{SNR} + \frac{1.5}{(SNR)^2} \right\}^{\frac{1}{2}} \quad (1)$$

where B_c = doppler filter bandwidth and SNR = signal-to-thermal noise ratio. This is also the expression used in the Dornier Analysis.

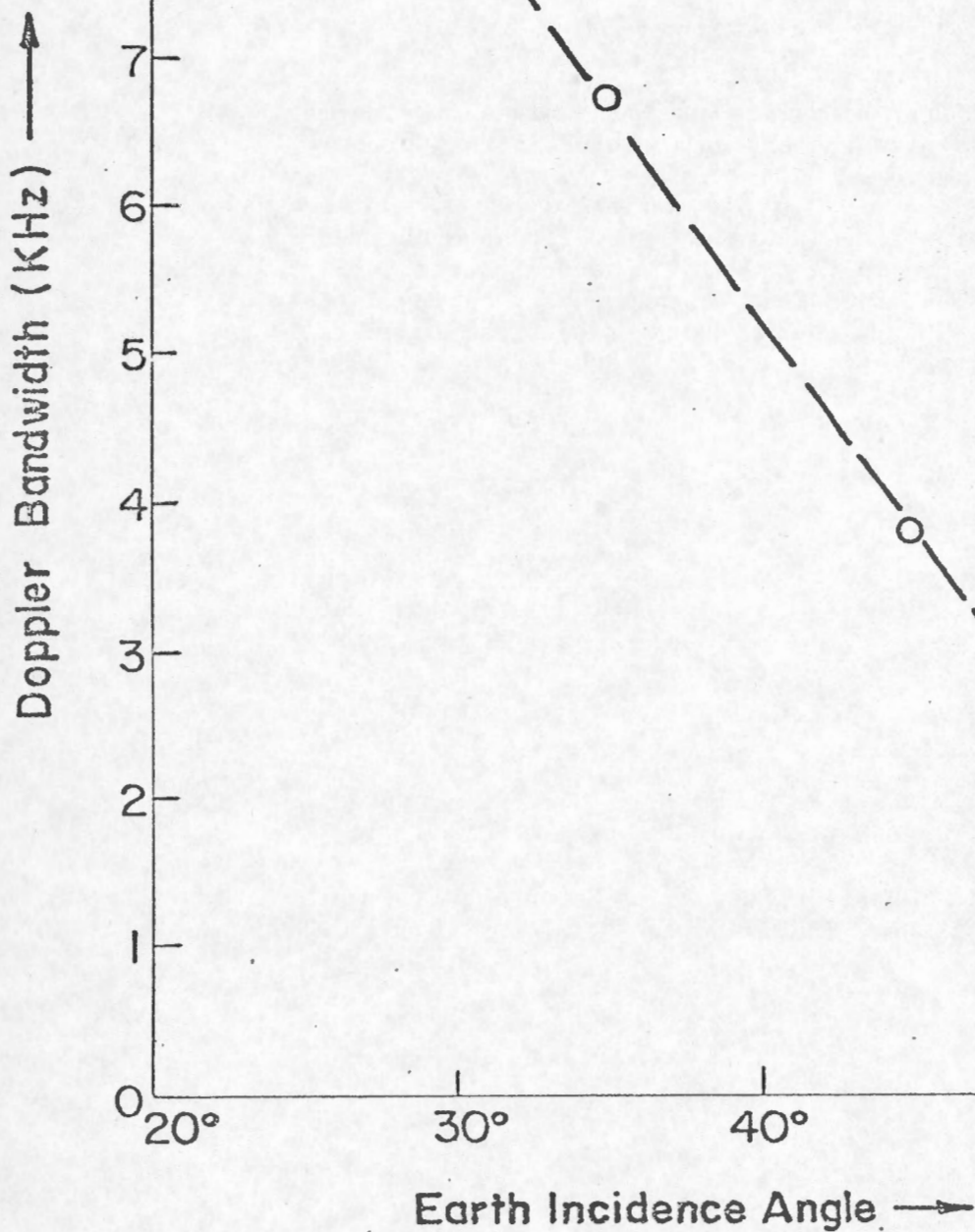
When SNR is large $K_p \rightarrow 1/(B_c \tau_{sn})^{\frac{1}{2}}$ and, (because the radar return signal is assumed to be a Gaussian random process, $(B_c \tau_{sn})$ is a measure of the number of independent samples making up the estimate of σ^0 . $(B_c \tau_{sn})^{-1}$ is then proportional to the 'speckle' inherent in the measurements and should, in general, be as small as possible.

² "An Operational Satellite Scatterometer for Wind Speed Measurements over the Ocean" by Grantham et al. 1975. NASA TM X-72672

³ "Standard Deviation of Scatterometer Measurements from Space", R.E. Fischer, IEEE, GE-10, No. 2, pp. 106-113, 1972.

DOPPLER BANDWIDTH vs INCIDENCE ANGLE

Altitude = 650 km
Azimuth Beam Width = $.8^\circ$
Ground Cell 50x50 km
 $V_g = 6.84 \text{ km sec}^{-1}$

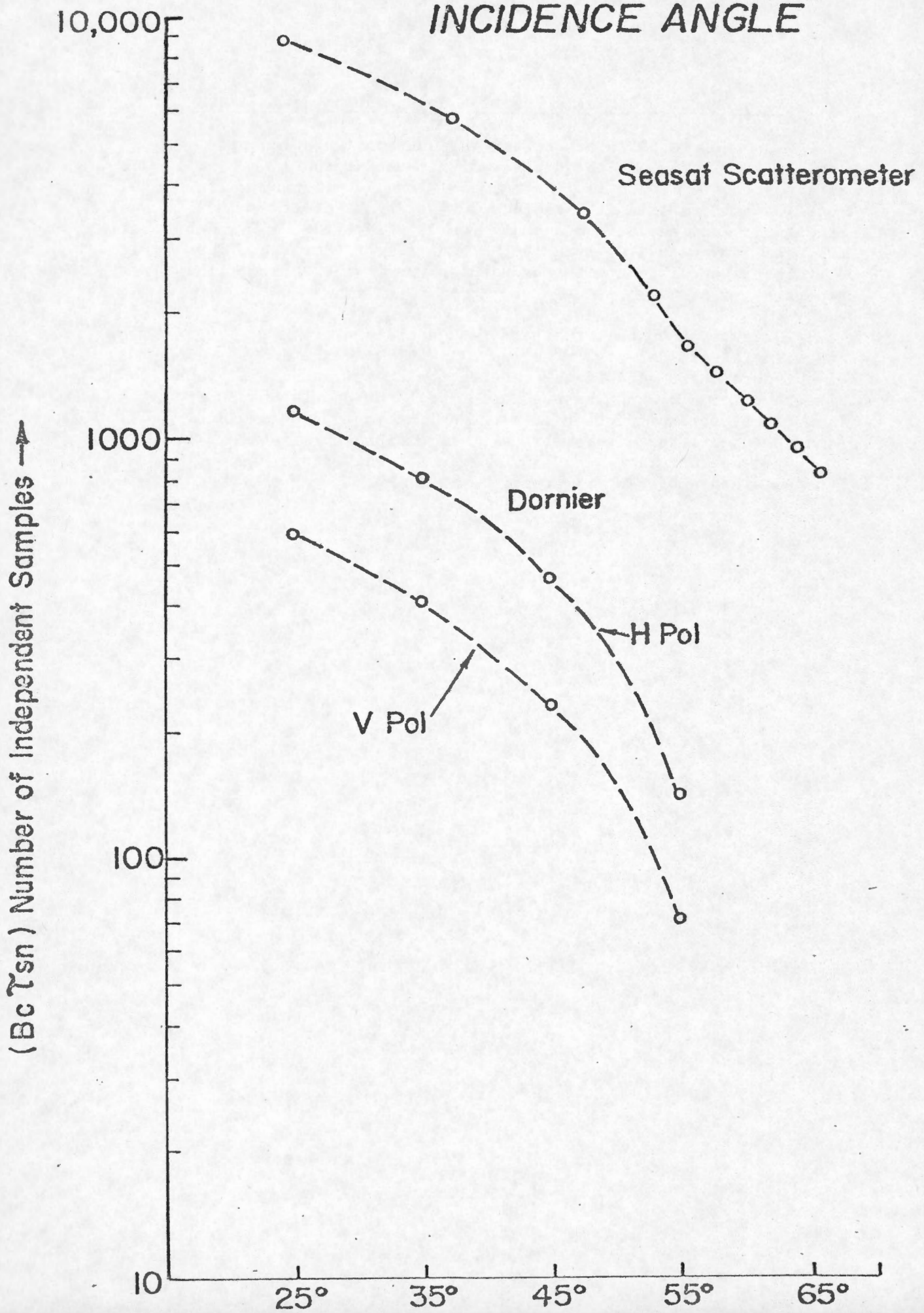


2) Doppler Bandwidth as a Function of Earth Incidence Angle

In order to calculate K_p for various configurations it is necessary to calculate the doppler filter bandwidth B_c in Eqn. 1 as a function of earth incidence angle. Even neglecting earth rotation effects this is a tedious but straight-forward calculation and has been done only for $\theta_i = 25^\circ, 35^\circ, 45^\circ$ and 55° . The equations used are given in the NASA report (Ref. 2). The 55° B_c value is consistent with the value given in the Dornier final report.

Graph 1 shows that the bandwidth decreases from approximately 10 KHz at 25° to approximately 1.2 KHz at 55° . Some of the parameters used in the calculation are given on the graph. Note that for a 50 x 50 km resolution cell the doppler bandwidth is a fairly strong function of ϕ the azimuth antenna beamwidth. Also it appears that it is virtually impossible to maintain a 50 x 50 km ground footprint with a 0.8° azimuth beamwidth at an incidence angle of 60° or larger.

NUMBER OF LOOKS vs INCIDENCE ANGLE



3) Number of Independent Samples as a function of θ_i .

Graph 2 shows the number of independent samples or "looks" versus earth incidence angle for the SEASAT scatterometer and for the V and H pol of the Dornier design. Even allowing for the (13.9/5.3) frequency factor in the doppler bandwidths the comparison between the SEASAT and Dornier system shows that the Dornier System is not as good. There are 2 reasons for this:

- 1) Because of the length restriction on the antenna the smallest azimuth beamwidth is given by an unweighted antenna 3.6 m in length $\phi_a = (51 \times .0566)/3.6$ degrees = 0.8° (as in Dornier report) whereas the SEASAT SASS used $\phi_a = 0.5^\circ$. Graph 3 (from Ref. 2 the NASA report) shows that to maintain the same value of K_p that the power required increases significantly as the azimuth beamwidth increases, this is due partly to the decrease in B_c required to maintain a 50 km resolution cell.
- 2) The length of the transmitted pulse should be just less than the 2-way propagation time of the nearest point in cell 1 in order to maximize the $(B_c \tau_{SN})$ product. However, because the peak power of the TWTA for the wind mode must be compatible with the wave (SAR) mode only a fraction (.72 m sec) of the total available time (~4.7 m sec) is used in the present design, which is relatively inefficient as a consequence. Note also that any attempt to extend operation of the C-band Doppler Scatterometer beyond 55° incidence angle will be difficult unless the ground cell size is increased.

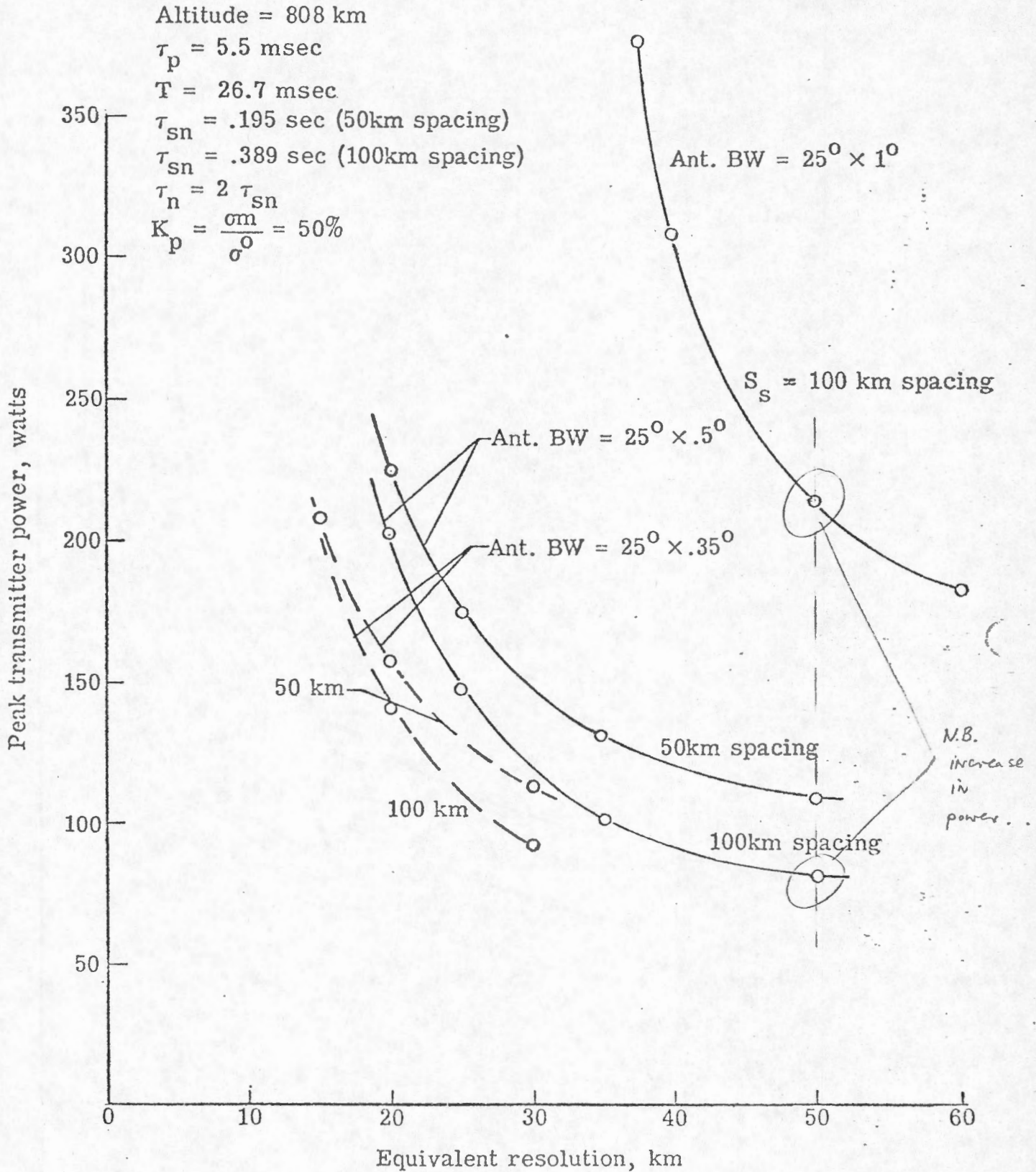
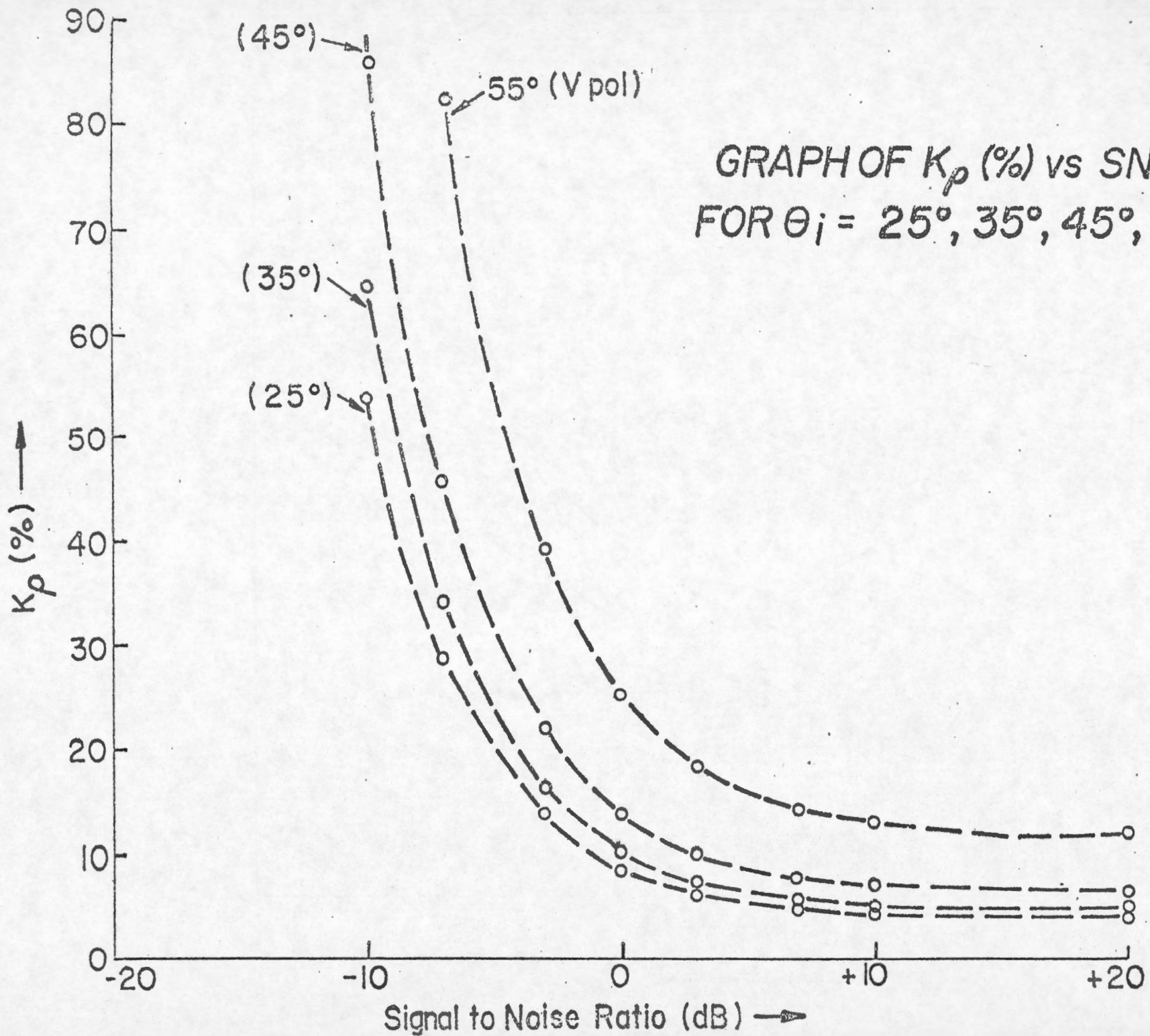


Figure 28.- Transmitter power requirements for fan beam scatterometer.

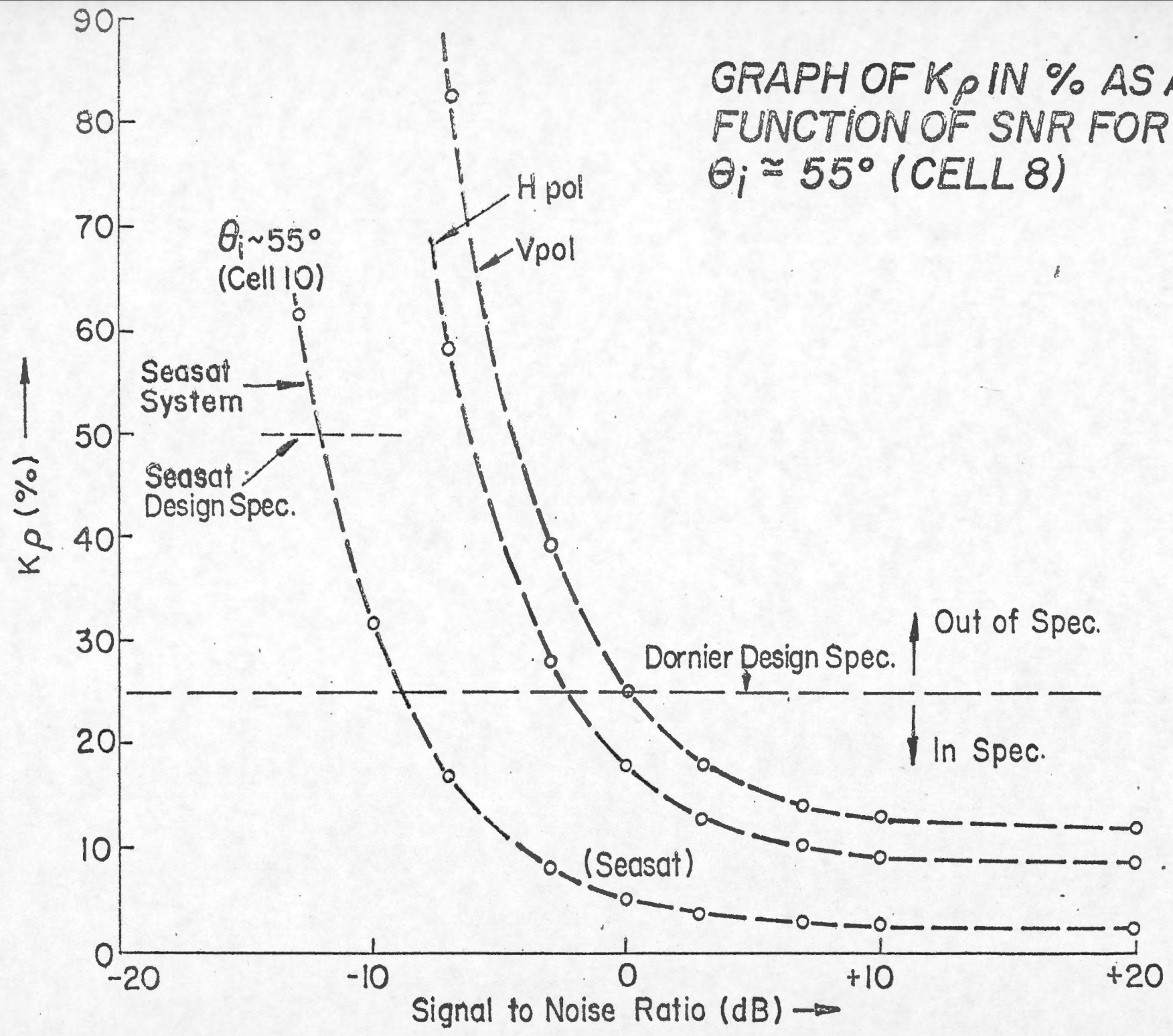


4) K_p as a Function of SNR

Given the values of $(B_c \tau_{sn})$ calculated as a function of incidence angle it is possible to calculate K_p as a function of SNR for different incidence angles.

Graph 4 shows that for positive SNR the accuracy in σ^0 measurement is dominated by the speckle term and that, as is obvious, the worst angle is 55° . All four curves have been calculated for V polarization. Below SNR = 0 dB thermal noise effects dominate and the Dornier design figure of $K_p < 25\%$ is satisfied for SNR > 0 dB (55°) and SNR > -5 dB for $\theta_i = 25^\circ$.

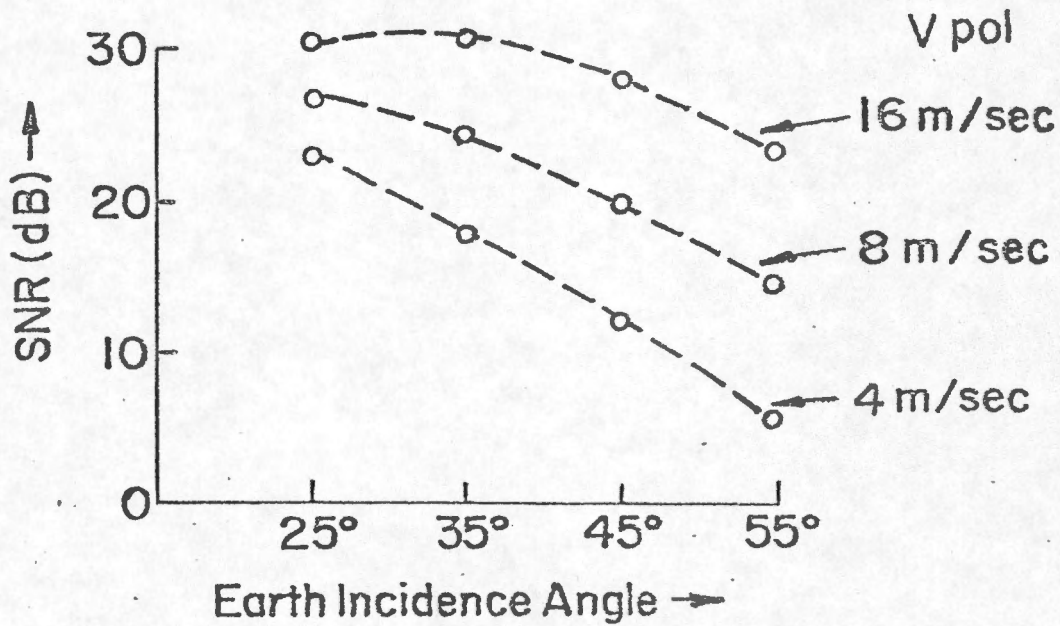
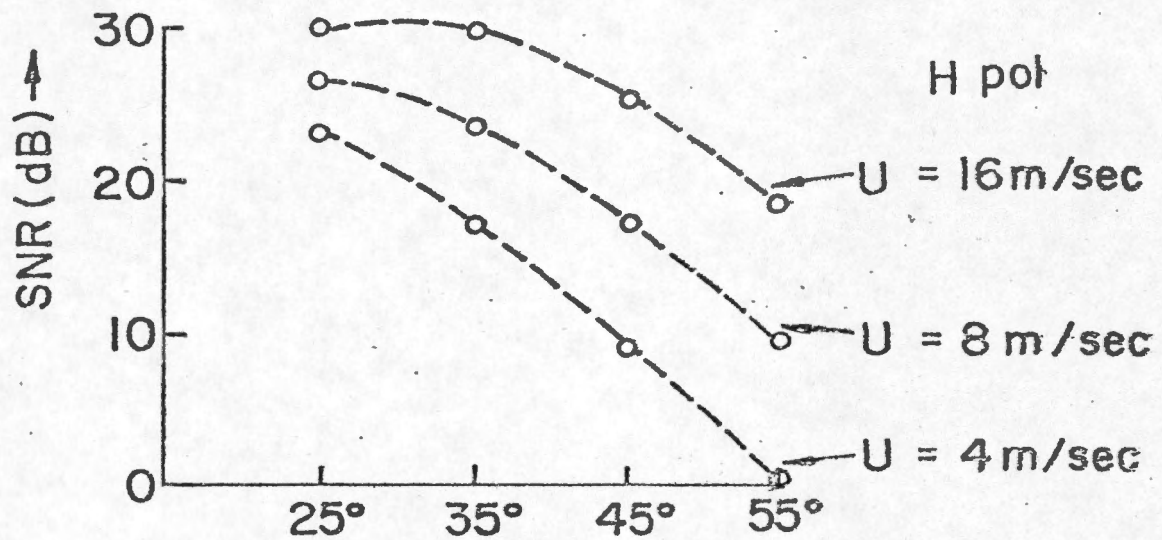
GRAPH OF K_p IN % AS A FUNCTION OF SNR FOR $\theta_i \approx 55^\circ$ (CELL 8)



5) K_p for V and H Pol. ($\theta_i = 55^\circ$), comparison with SEASAT.

Graph 5 shows the comparison between Dornier cell 8 ($\theta_i = 55^\circ$) V and H pol and SEASAT scatterometer cell 10 ($\theta_i \sim 55^\circ$) measurements. Note that the increased incoherent averaging for the SEASAT scatterometer allows comparable σ^0 measurements with SNR = -9 dB (SEASAT), SNR = -2.5 dB (Dornier H pol) and SNR = 0 dB (Dornier V pol).

SNR vs θ_i



6) SNR as a function of θ (wind speed, $u^* = 4, 8, 16 \text{ m sec}^{-1}$).

Using
$$P_r = \frac{P_t \left(\frac{G}{G_0}\right)^2}{4\pi R_c^3 \phi \beta^2} \cdot \sigma^0 \cdot \lambda^2 \cdot \epsilon^2 \cdot L \cdot L_s$$

and $SNR = P_r / K T_s B_c$

where P_t = transmitted power, 1667 watts

G/G_0 = relative antenna gain

λ = wavelength 0.0566 m

ϵ = antenna efficiency

L = doppler cell length

L_s = total system losses

R_c = range to cell

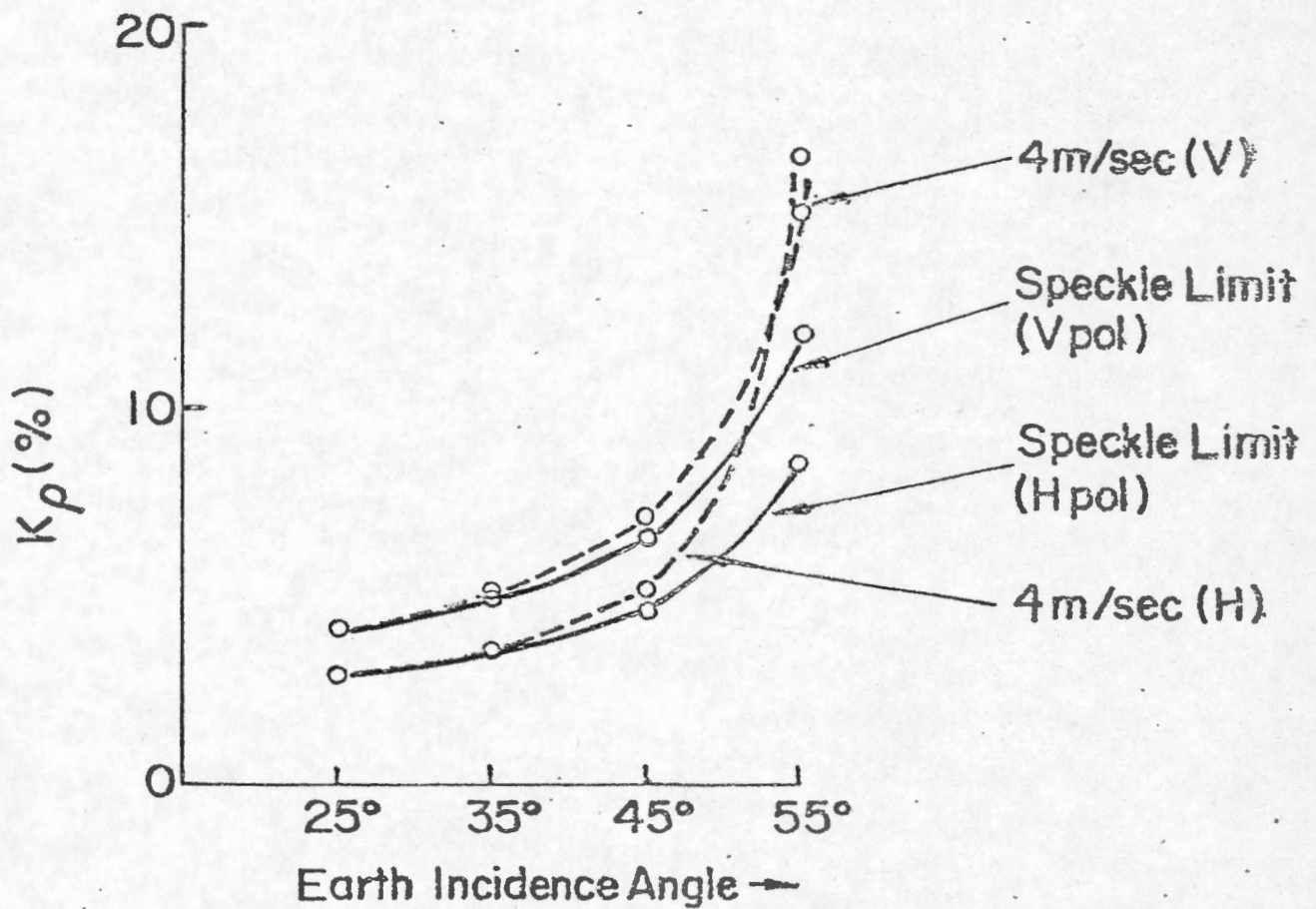
$SNR = \frac{K G_0^2 \cdot \sigma^0 \cdot L}{R_c^3 \cdot B_c}$ where K is independent of θ_i

Estimates based on these expressions leads to graph 6. Note that these curves have been calculated using (crosswind) σ^0 values from the Wentz (14.9 GHz) model, however, the worst case link budget calculation (H, 4 m sec^{-1} , 55°) given in the Dornier report is consistent with the appropriate value in these curves. The following values were used for the antenna $\phi_a = .8^\circ$, $\beta = 33^\circ$, $G/G_0:25^\circ = -4.5 \text{ dB}$, $G/G_0:35^\circ = -7 \text{ dB}$, $G/G_0:55^\circ = -6 \text{ dB}$.

Graph 6 shows that $u^* > 4 \text{ m sec}^{-1}$ the system will operate with a positive SNR. Crosswind σ^0 values have been used from the Wentz model in all the graphs. It is also apparent that optimum illumination in elevation has not been used. By increasing the elevation aperture one could increase the peak gain by a few dB and consequently save a few dB in power. Although this would make a significant difference to the $(G/G_0:25^\circ)$ values the SNR margin is sufficient to allow for a $(G/G_0:25^\circ)$ reduction of ~5-10 dB.

K_p vs θ_i

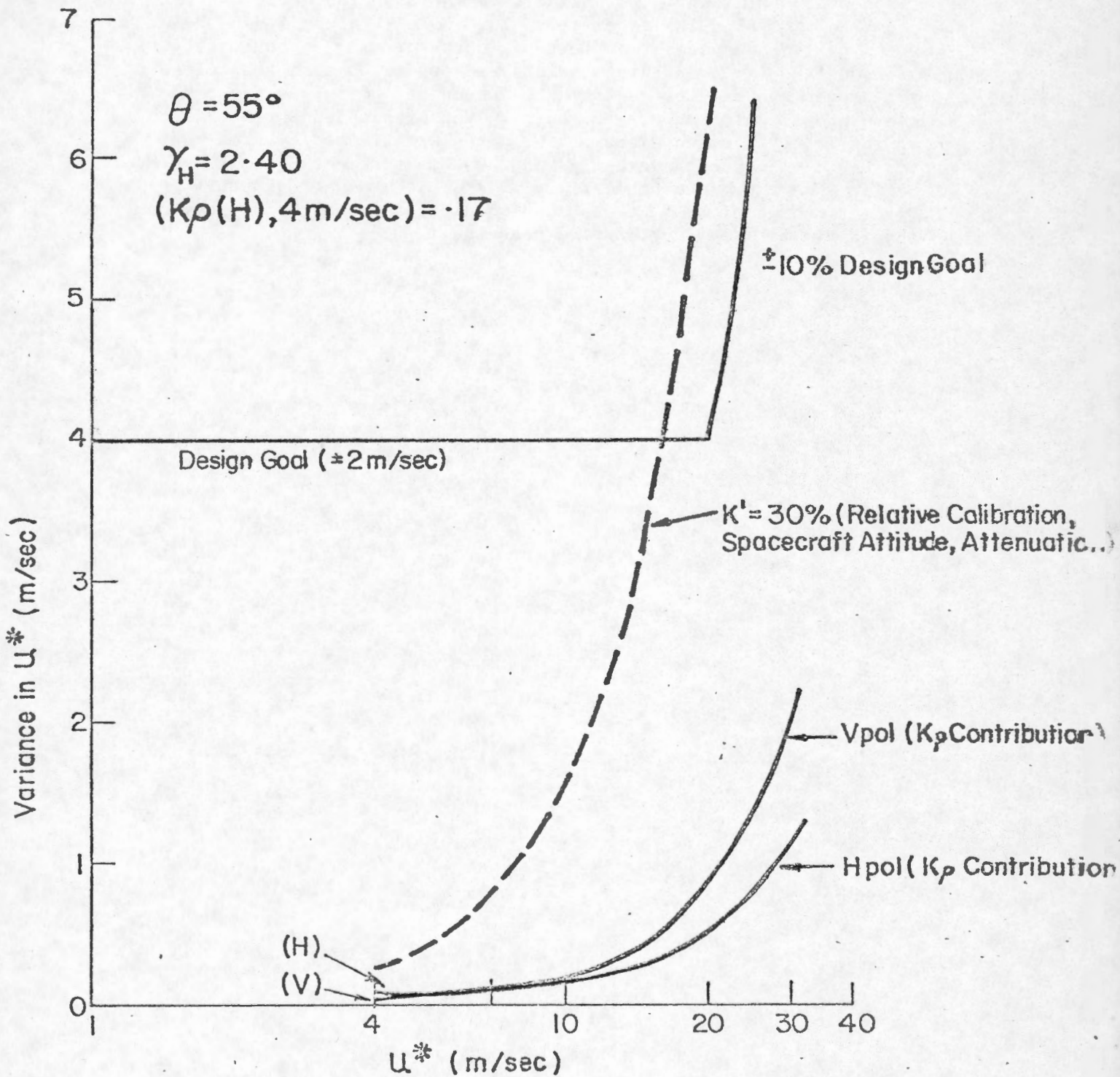
FOR $U^* = 4 \text{ m/sec}$ (V and H)
AND U^* LARGE (ie. MEASUREMENT
LIMITED BY SPECKLE NOISE



7. K_p as a function of θ_i .

Graph 7 shows the normalized standard deviation in σ^0 as a function of θ_i . Two curves are drawn for $u^* = 4 \text{ msec}^{-1}$ (crosswind) for V and H polarization. For most incidence angles the V pol K_p value is larger than the H pol K_p value, i.e., the H pol σ^0 measurement is better. Only for $\theta_i >$ approximately 52° does the larger SNR values for V measurements more than offset the poorer averaging of using half the number of pulses for a V measurement as for an H measurement. For wind speeds greater than approximately 8 m sec^{-1} the measurements are limited by the available incoherent averaging and the H measurements are always better than the V measurements. It is debatable whether the Dornier scheme of 84 V pulses and 168 H pulses would be any better than a simple 126:126 V:H pulse sequence.

VARIANCE IN U^* vs U^*



8) Standard Deviation in u^* as a function of σ^0 and u^*

Using the simple model $\sigma^0 = a(u^*)\gamma$ for average backscatter to wind speed (u^*) dependence and neglecting azimuthal variation we obtain

$$du^* = \frac{u^*}{\gamma} \left\{ \frac{d\sigma^0}{\sigma^0} - \frac{da}{a} - \gamma \ln u^* \frac{d\gamma}{\gamma} \right\}$$

where $d\sigma^0$ = error in σ^0 , etc.

and

$$\text{VAR}(u^*) = \frac{(u^*)^2}{\gamma^2} \left\{ \frac{\text{VAR}(\sigma^0)}{\sigma^0^2} + \frac{\text{VAR}(a)}{a^2} - \frac{(\gamma \ln u)^2}{\gamma^2} \text{VAR}(\gamma) \right\}$$

where $\text{VAR}(u^*)$ = Variance in u^* etc.

$$= \frac{(u^*)^2}{(\gamma)^2} \left\{ (K_p^2 + K'^2) + \frac{\text{VAR}(a)}{a^2} + (\gamma \ln u)^2 \frac{\text{VAR}(\gamma)}{\gamma^2} \right\}$$

Where K'^2 = Variance in measurements of σ^0 due to instability in relative calibration, variation in atmospheric attenuation, spacecraft attitude, etc.

Ignoring the problems related to uncertainties and uniqueness of the wind speed model (i.e. a and γ) we have

$$\text{VAR}(u^*) = \left(\frac{u^*}{\gamma} \right)^2 (K_p^2 + K'^2)$$

Graph 8 is an attempt to illustrate the contribution to the variance in u^* from uncertainties due to thermal noise and speckle (both contained in the K_p term) and the relative calibration and attenuation term (K'). Graph 8 shows that at the low wind speeds where the desired relative accuracy is low (i.e. ± 2 m/sec at winds up to $\sim 10 \text{ msec}^{-1}$) that the contribution to the u^* error (variance) budget from K_p is very small. Guessing a value of 30% for relative calibration, sc attitude and attenuation problems leads to the curve plotted for the resulting contribution to the u^* variance.

These curves show that the Dornier design goal of a $K_p < 25\%$ for low winds appears to be unnecessarily stringent. Designing to a $K_p < 50\%$ (as was done for the SEASAT scatterometer) would save power and lead to a marginal decrease in accuracy of u^* estimation at low wind speeds and no difference at moderate or high wind speeds. Clearly this analysis does not begin to examine the effect on wind direction extraction. In respect to the SEASAT results it is interesting to note that the worst case (low wind speed) system design was based on ϕ values which appear to be much larger than the currently accepted values. Consequently, the poorer performance of the SEASAT scatterometer at low winds may be due to the fact that the K_p value was at times larger than their design spec of $K_p < 50\%$. In practice ϕ estimates were rejected in the SASS processing if the K_p values were too large. It appears from Graph 8 that a worst case $K_p < 50\%$ is adequate and that the Dornier spec of $K_p < 25\%$ could be relaxed.

9) Conclusions and Comments

- 1) The proposed wind mode scatterometer is inefficient in power* because the combination of a low resolution wind mode and the relatively high resolution wave mode appears to lead to an inefficient design for the wind mode. The peak and average power required for the Dornier design are ~ 16 times and ~ 2 times that used on SEASAT respectively, although one would expect a lower power requirement at the lower frequency.
- 2) The Dornier design aims for a $K_p < 25\%$ and it follows from this work and the Dornier report that the worst case value is approximately 17%. It appears that this could be relaxed without appreciably degrading the recovery accuracy in u^* . The effect on wind direction extraction accuracy is hard to estimate without more simulation work.
- 3) The elevation beamwidth quoted (33°) does not appear to be optimum and a few dB in power may be saved by decreasing the beamwidth and increasing the peak gain.
- 4) The relatively poor incoherent averaging (for a spaceborne scatterometer!) arises partly because of the short (.72 msec) pulse length which is necessary because of TWT operation limitations. The finite pulse length leads to a transmitted power spectrum which is not a delta function but rather has a bandwidth of order 1.4 KHz, ie. comparable to the doppler filter bandwidth of the 55° cell (~ 1.2 KHz). It is not clear that the complications arising from this effect have been considered.
- 5) Because of the power requirements of the wind mode, the other modes of a combined active microwave instrument may be compromised because of spacecraft power limitations.
- 6) Although it has been suggested above that K_p could be increased, this should not be done at the expense of the available incoherent averaging; i.e. neither B_c nor τ_{sn} should be decreased. High wind speed performance may be improved slightly by equating the number of looks for V and H pol transmission.

* One development which may alleviate this problem is the current research going on with multistage collector TWT's which can be used with variable output powers (Multimode Travelling Wave Amplifier Tubes, E. Buck Microwave Journal Feb. 1981, p 65).

GSC/CGC OTTAWA



00G 02875748